Crystal Structure of a Deacylation-defective Mutant of Penicillin-binding Protein 5 at 2.3-Å Resolution*

Christopher Davies‡, Stephen W. White§¶, and Robert A. Nicholas‖**

From the ‡School of Biological Sciences, University of Sussex, Falmer, Brighton BN1 9QG, United Kingdom, §Department of Structural Biology, St. Jude Children's Research Hospital, Memphis, Tennessee 38105, ¶Department of Biochemistry, University of Tennessee, Memphis, Tennessee 38163, and ‖Department of Pharmacology, University of North Carolina at Chapel Hill, Chapel Hill, North Carolina 27599-7365

Penicillin-binding protein 5 (PBP 5) of *Escherichia coli* functions as a D-alanine carboxypeptidase, cleaving the C-terminal D-alanine residue from cell wall peptides. Like all PBPs, PBP 5 forms a covalent acyl-enzyme complex with β-lactam antibiotics; however, PBP 5 is distinguished by its high rate of deacylation of the acyl-enzyme complex ($t_{1/2} \sim 9$ min). A Gly-105 → Asp mutation in PBP 5 markedly impairs this β-lactamase activity (deacylation), with only minor effects on acylation, and promotes accumulation of a covalent complex with peptide substrates. To gain further insight into the catalytic mechanism of PBP 5, we determined the three-dimensional structure of the G105D mutant form of soluble PBP 5 (termed sPBP 5′) at 2.3 Å resolution. The structure is composed of two domains, a penicillin binding domain with a striking similarity to Class A β-lactamases (TEM-1-like) and a domain of unknown function. In addition, the penicillin-binding domain contains an active site loop spatially equivalent to the Ω loop of β-lactamases. In β-lactamases, the Ω loop contains two amino acids involved in catalyzing deacylation. This similarity may explain the high β-lactamase activity of wild-type PBP 5. Because of the low rate of deacylation of the G105D mutant, visualization of peptide substrates bound to the active site may be possible.
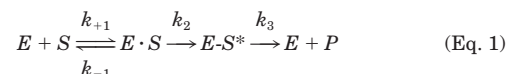
Penicillin and other β-lactam antibiotics exert their lethal effect by inhibiting the proteins that synthesize bacterial cell wall peptidoglycan (1). These proteins, known as penicillin-binding proteins or PBPs,[1] utilize lipid-linked disaccharide peptide substrates to catalyze both the polymerization of glycan chains (transglycosylation) and cross-linking of peptide chains (transpeptidation) during cell wall synthesis. In the latter reaction, a serine residue on the PBP reacts with the acyl-D-Ala-D-Ala C terminus of the peptide chain to form a transient acyl-enzyme complex, releasing the C-terminal D-alanine residue. This complex reacts with an amino group from another peptide chain to form a cross-link, which is crucial to the integrity and rigidity of the cell wall. An additional activity catalyzed by some PBPs, carboxypeptidation, occurs when the acyl-enzyme complex reacts with water. Penicillin and other β-lactam antibiotics mimic the structure of the acyl-D-Ala-D-Ala C terminus of the peptide chain (2) and react with PBPs to form an acyl-enzyme complex. Unlike the transient nature of the PBP-peptide complex, the acyl-enzyme complex formed between PBPs and β-lactam antibiotics is much more stable and results in prolonged inhibition of the enzyme.

In *Escherichia coli*, at least 10 PBPs have been identified. These PBPs can be split into two classes: the high molecular mass PBPs (PBPs 1A, 1B, 1C, 2, and 3) and the low molecular mass PBPs (PBPs 4, 5, 6, 6b, and 7) (3). High molecular mass PBPs are essential for cell viability and are involved in the physiological processes of cell elongation, cell division, and the maintenance of cell shape (4). The role of low molecular mass PBPs in bacterial physiology is less clear. These PBPs catalyze D,D-endopeptidase or D,D-carboxypeptidase activity both *in vitro* and *in vivo* (5, 6), but although they account for >90% of the amount of penicillin G bound to membranes, they are not essential for cell viability (7). However, a recent study utilizing strains with multiple deletions of low molecular mass PBPs revealed a role for PBP 5 in the proper synthesis of peptidoglycan (8).

Production of a β-lactamase is the most common mechanism by which bacteria become resistant to β-lactam antibiotics (9). The initial step of the reaction catalyzed by these enzymes is analogous to that mediated by PBPs, but instead of accumulating a stable acyl-enzyme complex, β-lactamases destroy the antibiotic by rapidly hydrolyzing the acyl-enzyme bond. Analysis of the sequences and crystal structures of PBPs and Class A and class C β-lactamases reveals strong structural similarities in the two classes of penicillin-interacting proteins (10–12). The hallmark of all active site serine-based penicillin-interacting proteins is the presence of three well conserved motifs in the active site (13). These motifs are the S*XX*K tetrad containing the active site serine residue, the (S/Y)*X*N triad, and the KT(S)G triad.

The reaction mechanism of the interaction of β-lactam antibiotics with PBPs and β-lactamases is represented schematically by the following three-step model.

$$E + S \underset{k_{-1}}{\overset{k_{+1}}{\rightleftharpoons}} E \cdot S \overset{k_2}{\longrightarrow} E\text{-}S^* \overset{k_3}{\longrightarrow} E + P \qquad \text{(Eq. 1)}$$

where E is the PBP or β-lactamase, S is a β-lactam antibiotic, $E \cdot S$ is the Michaelis complex, $E\text{-}S^*$ is the covalent acyl-enzyme complex, and P is the inactive degradation product (14, 15). In PBPs, k_3 is usually quite small compared with k_2, leading to

---

[1] The abbreviations used are: PBP, penicillin-binding protein; sPBP, soluble PBP; CPase, carboxypeptidase; MIR, multiple isomorphous replacement; r.m.s., root mean square.

accumulation of the inactive acylated enzyme. For β-lactamases, both the k_2 and k_3 rate constants are very large, and the β-lactam antibiotic is hydrolyzed.

In contrast to most other PBPs, *E. coli* PBP 5 is distinguished by its high β-lactamase activity, with $k_3 \approx 0.07$ s^{-1} ($t_{1/2} < 10$ min) for the penicilloyl-PBP 5 complex. A mutant PBP 5, PBP 5-G105D (termed PBP 5′), shows near normal acylation rates with penicillin G but displays a 30-fold decrease in the rate of deacylation (16, 17). Additionally, the mutant protein forms a stable covalent complex with the depsipeptide substrate, *N,N′*-diacetyl-L-lysyl-D-alanyl-D-lactate, which is not observed with the wild-type protein (16). The phenotype of PBP 5′ is similar to that of wild-type PBP 5 in which Cys-115 has been modified with sulfhydryl reagents, causing a larger effect on deacylation than acylation (18). However, since the mutants PBP 5-C115A and PBP 5-C115S both display wild-type levels of D-alanine carboxypeptidase (CPase) and penicillin binding activities, this residue does not appear to be directly involved in the catalytic mechanism of the enzyme (17). Subsequent attempts to identify residues involved in deacylation of PBP 5 have been unsuccessful (19).

In an effort to understand the molecular mechanism of deacylation of PBP 5 and to define further the interactions of β-lactam antibiotics and peptide substrates with PBPs, we have solved the structure of the G105D mutant of PBP 5 at 2.3-Å resolution, the first structure for PBP 5. It reveals the closest similarity yet identified between a PBP-type enzyme and a Class A β-lactamase, which may explain the relatively high β-lactamase activity of PBP 5.

MATERIALS AND METHODS

Protein Purification and Crystallization—Construction of the expression plasmid encoding sPBP 5′ has been described (17, 20). The gene encoding the G105D mutant form of PBP 5 missing its last 17 codons (plus six extra codons added during plasmid construction) was cloned into the *Pst*I-*Hin*dIII restriction sites of pBR322. Overnight cultures of MC1061 harboring the expression plasmid were subjected to osmotic shock (21), and sPBP 5′ was purified from the shock fluid by ampicillin affinity chromatography exactly as described (17). The purified protein was dialyzed exhaustively against 20 mM Tris· HCl, 150 mM NaCl, 10 mM 2-mercaptoethanol, 0.2% NaN$_3$, pH 7.5 and concentrated to 6−8 mg ml^{-1}. SDS-polyacrylamide electrophoresis indicated that the protein was >98% pure with very little of the characteristic 30- and 10-kDa breakdown products (22).

Crystallization conditions were similar to those described previously (23). Crystals were grown by vapor diffusion in 20% polyethylene glycol 4000, 50 mM Tris·HCl, pH 7.0, 0.2% NaN$_3$. Crystals of bullet-shaped morphology formed at 18 °C within 1–2 days. The crystals belong to space group P3$_2$ with cell dimensions $a = 50.83$ Å and $b = c = 140.29$ Å. There is one molecule in the asymmetric unit.

Data Collection—In all cases crystals were mounted in quartz capillaries, and data were collected at room temperature by the standard oscillation method. The initial native data set was collected using a Rigaku RAXIS-II image plate system (Molecular Structures Corp., The Woodlands, TX) mounted on a Rigaku RU-300 x-ray generator operating at 40 kV and 80 mA and fitted with a graphite monochromator. The crystal-to-plate distance was 130 mm, the oscillation angle was 3°, and the exposure time was 30 min frame^{-1}. A total of 84° of data was collected.

Derivative diffraction data were collected using a DIP 2030H image plate detector mounted on a Nonius FR391 rotating anode x-ray generator fitted with MacScience focusing mirrors (Nonius B. V., Delft, The Netherlands) and operating at 40 kV and 100 mA. Data were collected at a crystal-to-plate distance of 150 mm, with an oscillation angle of 1° and an exposure time of 18 min frame^{-1}. Rotation ranges of 60–75° were sufficient to collect essentially complete data sets.

For model refinement purposes a high resolution data set was collected, where the crystal-to-plate distance was 150 mm, the oscillation angle was 1°, and the exposure time was 12 min frame^{-1}. To ensure a high redundancy of data, the crystal was rotated through a total of 90°. In all cases the oscillation data were processed using HKL (24). In the case of derivative data, the Friedel pairs were not merged in order to retain the anomalous signal.

Phasing—A search for derivatives was made by soaking crystals in solutions of heavy atom compounds in stabilizing buffer (20% polyethylene glycol 4000 in 100 mM Tris·HCl, pH 7.0). Soaks in various mercury and platinum compounds yielded several promising derivatives, as judged by difference Patterson maps. In each case heavy atom positions

TABLE I
Data collection statistics
Hg(CN)$_2$, mercury (II) cyanide; PIP, di-μ-iodobis(ethylenediamine) di-platinum nitrate.

	Native 1	Native 2	Hg(CN)$_2$	PIP
Molarity (mM)			1	10/sat.
Length of soak			2 d	1 h
Temperature (K)	298	298	298	298
Reflections (unique)	13776	17239	13482	9584
Reflections (measured)	37497	43406	34123	18341
Completeness (%)	98.0	94.8	95.6	95.9
Resolution (Å)	2.5	2.3	2.5	2.8
R_{SYM}[a]	7.9	6.9	7.4	9.1

^{a} $R_{SYM} = \dfrac{\Sigma|I_l - I_M|}{\Sigma I_M}$, where I_l is the intensity of the measured reflection, and I_M is the mean intensity of all symmetry-related reflections.

TABLE II
Phasing statistics
Derivative abbreviations are as in Table I.

Derivative	Hg(CN)$_2$		PIP	
	Isomorphous	Anomalous	Isomorphous	Anomalous
Type of data	Isomorphous	Anomalous	Isomorphous	Anomalous
Resolution	2.5	2.5	2.8	2.8
No. of reflections	7246	5863	5182	4003
R_{MERGE}[a]	20.3		6.5	
Phasing power[b]	1.28	0.91	1.43	0.70
R_{CULLIS}[c]	0.849	0.946	0.777	0.971
R_{KRAUT}[d]	0.203	0.514	0.132	0.577
Overall figure of merit:				
Before solvent flattening		0.244		
After solvent flattening		0.933		

^{a} $R_{MERGE} = \dfrac{\Sigma|F_{PH} - F_P|}{\Sigma|F_{PH}|}$.

^{b} Phasing power $= \dfrac{F_H}{E_{r.m.s.}}$.

^{c} $R_{CULLIS} = \dfrac{\Sigma(F_{PH} \pm F_P) - F_H(calc)}{\Sigma|F_{PH} - F_P|}$.

^{d} $R_{KRAUT} = \dfrac{\Sigma|F_{PH}(obs) - F_{PH}(calc)|}{\Sigma F_{PH}(obs)}$. F_P, F_{PH}, and F_H are the protein, derivative, and heavy atom structure factors, respectively, and $E_{r.m.s.}$ is the residual lack of closure.
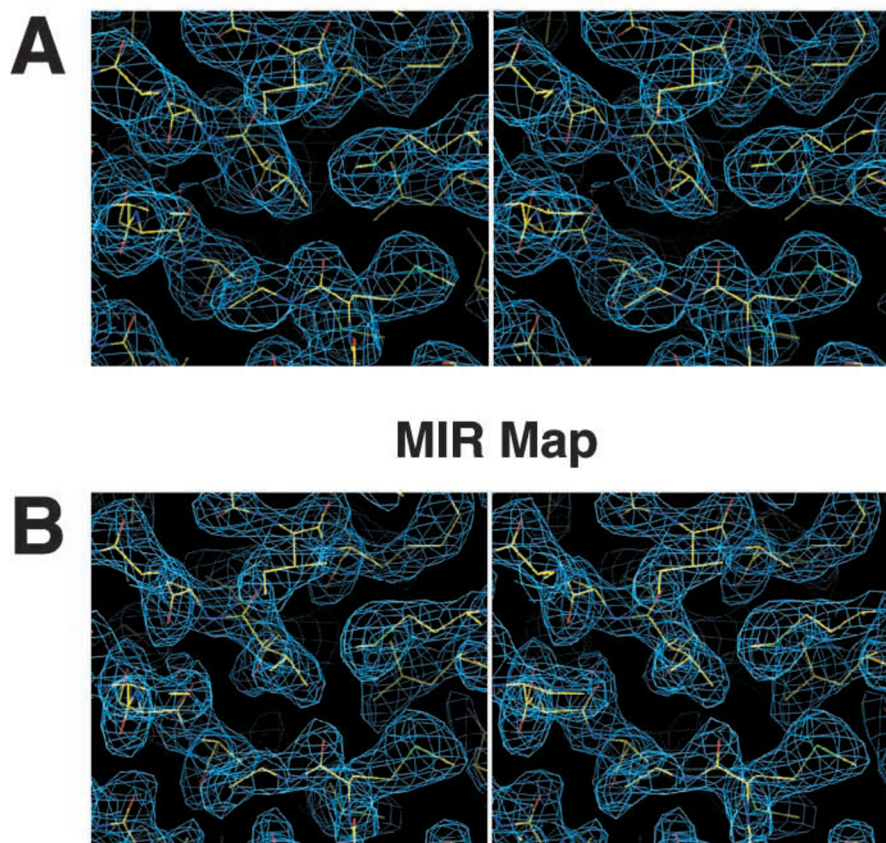
FIG. 1. **Stereoviews of the electron density maps of sPBP 5'.** *A*, the solvent-flattened MIR map at 2.5-Å resolution. *B*, the $2/F_o - F_c$ calculated phased map generated from the final refined coordinates at 2.3 Å. The region shown is a portion of the hydrophobic core in domain 1. Both maps are contoured at 1 σ and are displayed using O (29).

were determined and refined, and the data were used in trial phasing. These calculations showed that two derivatives, mercury cyanide ($HgCN_2$) and di-μ-iodobis-(ethylenediamine) di-platinum nitrate (PIP), were of the best quality and sufficient to solve the structure. All calculations to this point were performed using PHASES (25). At this stage the derivative and native data were merged using SCALEIT (26), and the final phasing calculation was performed using SHARP (27) and included anomalous data. The resulting multiple isomorphous replacement (MIR) phases were improved by solvent flattening using SOLOMON (28) with an estimated solvent content of 46%.

Model Building and Refinement—An MIR electron density map (Fig. 1*B*) was calculated using CCP4 programs (26) and displayed using the program O (29). The map was of excellent quality and was easily interpreted to build the entire structure, including side chains, with the exception of residues 1–3 and 74–90. The model was then refined by alternating rounds of XPLOR and manual revision using O. In later rounds water molecules were included. The final round of refinement was performed using REFMAC (26). The stereochemistry of the final model was evaluated using PROCHECK (30). The numbering of the final model corresponds to the sequence of the mature processed protein.

RESULTS

Structure Determination

The structure of sPBP 5' was determined by MIR with anomalous scattering. The data collection and phasing statistics are shown in Tables I and II, and portions of both the MIR and final $2/F_o - F_c$ electron density maps are shown in Fig. 1. The final structure has an *R* factor of 19.6% ($R_{free} = 27.0\%$) at 2.3-Å resolution (Table III). Currently 151 water molecules are included in the model.

As defined by PROCHECK (30), 90.0% of the residues lie within the most favored region of the Ramachandran plot. Three residues fall within disallowed regions. Of these, Ala-155

and Lys-219 both lie within loop regions with weak density, whereas Ile-212 is a hydrophobic core residue with excellent density. Residues with the highest B factors are located exclusively at the termini or in surface-exposed loops. Certain parts of the molecule have been omitted from the model where they correspond to regions of poor electron density, likely due to disorder. These are residues 1–3 at the N terminus, seven residues at the C terminus (six of which are non-native and result from the genetic construct), and an external loop comprising residues 74–90. The apparent flexibility of these latter residues is consistent with the increased susceptibility of the G105D mutant enzyme to proteolysis compared with PBP 5 wild type. Proteolysis of sPBP 5' generates characteristic 30- and 10-kDa fragments by cleavage between residues 87 and 88, which reside within this external loop (31).

Structure Description

sPBP 5' is composed of two domains that are oriented approximately at right angles to each other (Fig. 2). Each domain is formed from contiguous primary sequence, residues 3 to 262 for domain 1 and residues 263 to 356 for domain 2. The N-terminal region of sPBP 5' is a loop that extends away from domain 1 and makes a slight contact with domain 2 via Lys-6.

Domain 1—The principal feature of domain 1 is a five-stranded anti-parallel β sheet that forms the hydrophobic core. This is packed on one side by an extended loop at the N terminus, α10, and a loop connecting β8 and β9 that contains a small α helix (α9). The other side is comprised primarily of an array of seven α helices. In addition, there are three β hairpin-like structures, β3-β4, β5-β6, and β7-β8, one of which (β3-β4) contains the disordered residues 74–90. The active site of PBP

TABLE III
Statistics of the final model

Resolution range (Å)	15.0-2.3
Sigma cut-off applied	0.0
Number of reflections used in refinement	17,208
Percentage of reflections used in R_{FREE}	10.0
Completeness of data in resolution range (%)	95.4
Number of protein atoms	2,597
Number of water molecules	151
R factor (%)	19.6
Free R factor (%)	27.0
r.m.s. deviations from ideal stereochemistry	
Bond lengths (Å)	0.011
Bond angles (°)	2.936
Dihedrals (°)	24.73
Impropers (°)	2.552
Mean B factor (main chain) (Å^3)	39.29
r.m.s. deviation in main chain B factor (Å^3)	1.36
Mean B factor (side chains and waters) (Å^3)	39.18
r.m.s. deviation in side chain B factors (Å^3)	1.55
Ramachandran plot	
Residues in most-favored region (%)	90.0
Residues in additionally allowed regions (%)	8.3
Residues in generously allowed regions (%)	0.7
Residues in disallowed regions (%)	0.1

5 is located within this domain at the boundary of the five-stranded β-sheet and the helical array (see below). It is immediately apparent that domain 1 has the same fold as Class A and Class C β-lactamases (discussed below).

Domain 2—This domain, which is almost exclusively comprised of β structure, is a sandwich of two anti-parallel β sheets, one three-stranded and the other two-stranded. The two-stranded sheet is kinked at residues Gly-272 and Asp-293, causing the two sides of the sheet to be at right angles. The effect of this is to form a loose β barrel at the C-terminal end of the domain. Compared with domain 1, domain 2 has a relatively hydrophobic surface as judged by an electrostatic plot (data not shown), although none of these hydrophobic residues are particularly well conserved in other CPases. The significance of this apparent hydrophobicity and the role of this domain in the function of the protein are unknown. A search of the Protein Data Bank using the DALI server (32) revealed no genuine structural similarities to domain 2.

Domain Interface—Since the hydrophobic cores of domains 1 and 2 extend to include the domain interface and because this region has comparatively low B factors, significant movements between domains 1 and 2 seem unlikely, suggesting that the relative juxtaposition of the two domains is conserved.

Sequence Alignment to Other CPases and Secondary Structure Assignment

A Blast search of the GenBank™ data base with *E. coli* PBP 5 as a query sequence identified two other *E. coli* PBPs (PBP 6 and PBP 6b) and PBPs from *Salmonella typhimurium* and *Haemophilus influenzae* as its closest matches. Alignment of these PBPs is shown in Fig. 3 along with secondary structure assignments from the three-dimensional structure of sPBP 5′. As expected, the regions of highest identity reside in and around the conserved sequence motifs (shown in parentheses) associated with the active site in domain 1: residues 42–53 (Ser[44]-*X*-*X*-Lys[47]), residues 110–114 (Ser[110]-*X*-Asn[112]), and residues 210–217 (Lys[213]-Thr[214]-Gly[215]) (19). Two additional highly conserved regions, comprising residues 149–154 and 195–203, also are located in close proximity to the active site (see Fig. 4). In general, the residues in domain 2 are less conserved than domain 1, and most of the conserved residues are within the hydrophobic core.
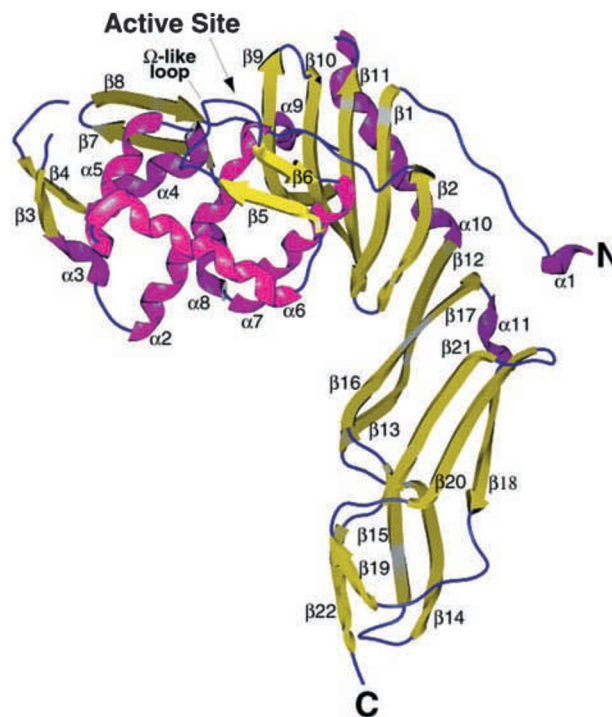

FIG. 2. **The structure of sPBP 5′.** The structure of sPBP 5′ with secondary structure assignments and the location of N and C termini are shown. In this view, the cytoplasmic membrane is at the bottom of the molecule, and the entrance to the active site is at the top. This figure was produced with the program SPOCK (available on the World Wide Web).

Active Site

The location of the active site is readily identified by plotting the conserved sequence motifs onto the sPBP 5′ structure. In common with other PBPs and β-lactamases, the active site is located in the cleft between the five-stranded anti-parallel β sheet and the large α helical cluster. As viewed in Fig. 2, the entrance to the active site is at the opposite end of the molecule from the C terminus and the membrane anchor (which is missing in our construct), in an ideal position to interact with cell wall peptides. The architecture of active site (Fig. 4) is comprised of the following elements: helix α2 (*yellow*), containing Ser-44 and Lys-47 of the S*XX*K tetrad; the turn between helices α4 and α5 (*green*), containing Ser-110 and Asn-112 of the SXN triad; and β9 (*orange*), the edge strand of the β sheet containing Lys-213, Thr-214, and Gly-215 of the KT(S)G triad. In addition, the loops between β5 and β6 and between β8 and α9 also contribute residues to the active site. These include His-151, present on the extended loop (*blue*) at the bottom of the cavity, and Arg-198, located on the loop (*purple*) at the top of the cavity. Both of these latter residues are conserved in related CPases (Fig. 4). The identification of Ser-44, Lys-47, Ser-110, Asn-112, and Lys-213 as active site residues is consistent with data showing that mutation of any of these renders PBP 5 highly deficient or, in some cases, completely inactive in both antibiotic binding and carboxypeptidation (19, 33).

The hydrogen-bonding network within the active site is extensive (Fig. 4). The ε-NH$_2$ group of Lys-47 plays a central role in this network, forming hydrogen bonds with the hydroxyl group of Ser-44, the amide carbonyl group of Asn-112, and the backbone carbonyl groups from both Ser-110 and His-151. In common with other penicillin-interacting enzymes, the ε-NH$_2$ group of Lys-213 forms a hydrogen bond with Ser-110. In contrast to Class A β-lactamases, in which two structurally conserved water molecules are typically observed within the

```
              10         20         30         40         50         60         70
              •          •          •          •          •          •          •
EcoPBP5  NIKTMIPGVPQIDAESYILIDYNSGKVLAEQNADVRRDPASLTKMMTSYVIGQAMKAGKFKETDLVTIGND
EcoPBP6  --AEQTVEAPSVDARAWILMDYASGKVLAEGNADEKLDPASLTKIMTSYVVGQALKADKIKLTDMVTVGRD
EcoPBP6b ENIPFSPQPPEIHAGSWVLMDYTTGQILTAGNEHQQRNPASLTKLMTGYVVDRAIDSHRITPDDIVTVGRD
HinPBP5  EDMQFGVTPPQITAQTYVLMDYNSGAILTALNPDQRQYPASLTKMMTSYVVGVALKQGKIHNTDMVTIGES
StyPBP5  DAVSFAPQPPAIDAGAWVLMDYTTGQVLTAGNEHQQRNPASLTKLMTGYVVDRAIDSHRISPDDIVTVGRD
             α1          β1         β2              α2              α3  β3

              80         90        100        110        120        130        140
              •          •          •     @    •    #     •          •          •
EcoPBP5  AWATGNPVFKGSSLMFLKPGMQVPVSQLIRGINLQSGNDACVAMADFAAGSQDAFVGLMNSYVNALGLKNT
EcoPBP6  AWATGNPALRGSSVMFLKPGDQVSVADLNKGVIIQSGNDACIALADYVAGSQESFIGLMNGYAKKLGLTNT
EcoPBP6b AWAKDNPVFVGSSLMFLKEGDRVSVRDLSRGLIVDSGNDACVALADYIAGGQRQFVEMMNNYAEKLHLKDT
HinPBP5  AWGRN---FPDSSKMFLDLNTQVSVADLNRGVIVVSGNDATVALAEHISGNVPNFVETMNKYVQQFGLKNT
StyPBP5  AWAKDNPVFVGSSLMFLKEGDRVSVRDLSRGLIVDSGNDACVALADYIAGGQPQFVAMMNSYVKKLNLQDT
                          β4   α4              α5              α6

             150        160        170        180        190        200        210
              •          •          •          •          •          •          •
EcoPBP5  HFQTVHGLDADGQYSSARDMALIGQALIRDVPNEYSIYKEKEFTFNGIRQLNRNGLLWDNSLNVDGIKTGH
EcoPBP6  TFQTVHGLDAPGQFSTARDMALLGKALIHDVPEEYAIHKEKEFTFNKIRQPNRNRLLWSSNLNEDGMKTGT
EcoPBP6b HFETVHGLDAPGQHSSAYDLAVLSRAIIHGEPEFYHMYSEKSLTWNGITQQNRNGLLWDKTMNVDGLKTGH
HinPBP5  NFTTPHGLDDPNQYSSARDMAIIGAHIIRDLPEEYKIYSEKNFTFNKIKQANRNGLLWDKTINVDGMKTGH
StyPBP5  HFETVHGLDAPGQHSSAYDLAVLSRAIIHGEPEFYHMYSEKSLTWNGITQQNRNGLLWDKTMHIDGLKTGH
          β5         β6      α7         α8      β7   β8    α9        β9

             220        230        240        250        260        270        280
              •          •          •          •          •          •          •
EcoPBP5  TDKAGYNLVASA-TEGQMRLISAVMGGRTFKGREAESKKLLTWGFRFFETVNPLKVGKEFASEPVWFGDSD
EcoPBP6  TAGAGYNLVASA-TQGDMRLISVVLGAKTDRIRFNESEKLLTWGFRFFETVTPIKPDATFVTQRVWFGDKS
EcoPBP6b TSGAGFNLIASA-VDGQRRLIAVVMGADSAKGREEEARKLLRWGQQNFTTVQILHRGKKVGTERIWYGDKE
HinPBP5  TSQAGYNLVASATTSNNMRLISVVMGVPTYKGREVESKKLLQWGFANFETFKTLEAGKEISEQRVYYGDKN
StyPBP5  TSGAGFNLIASA-VDGQRRLIAVVMGAKSSKGREEQARKLLQWGQQNFATVQILHSGKKVGSERIWYGDKE
            β10        β11           α10            β12 β13      β14

             290        300        310        320        330        340        350
              •          •          •          •          •          •          •
EcoPBP5  RASLGVDKDVYLTIPRGRMKDLKASYVLNSSELHAPLQKNQVVGTINFQLDGKTIEQRPLVVLQEIPEGN
EcoPBP6  EVNLGAGEAGSVTIPRGQLKNLKASYTLTEPQLTAPLKKGQVVGTIDFQLNGKSIEQRPLIVMENVEEGG
EcoPBP6b NIDLGTEQEFWMVLPKAEIPHIKAKYTLDGKELTAPISAHQRVGEIELYDRDKQVAHWPLVTLESVGEGS
HinPBP5  SVKLGALMDHFITIPKGKQSEVKARYELADKNLQAPLVKGQVIGKVVYQLDGKDIASANLQVMNDVGEAG
StyPBP5  KIALGTEQDFWMALPKAEIPHIKAKYVLDRKELEAPIAAHQQVGEIELYDRDKLIAQWPLVTLESVGKGG
          β15    β16 β17  α11  β18       β19        β20         β21        β22
```
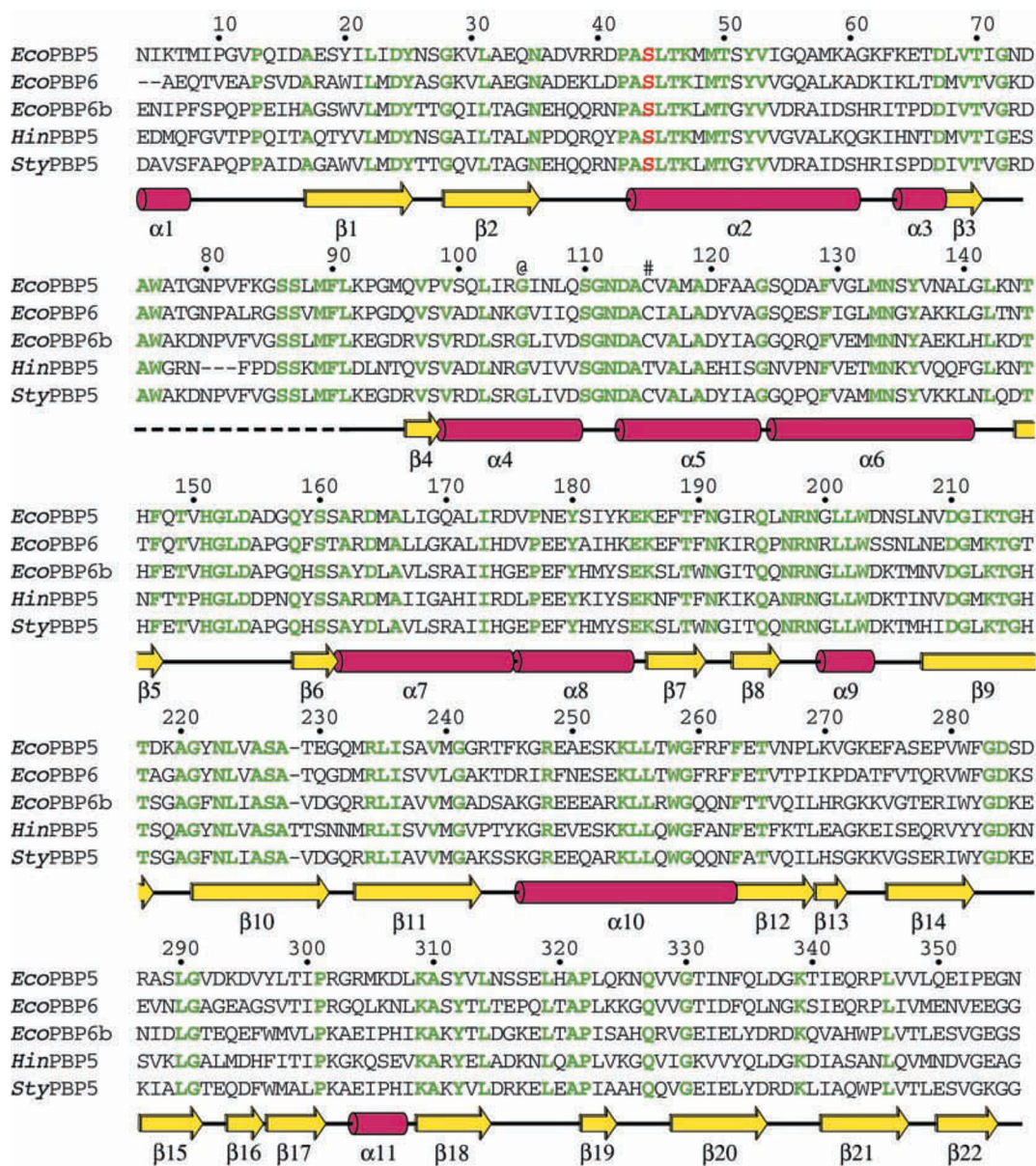
FIG. 3. **Sequence alignment and secondary structure assignment.** Alignment of the soluble, mature form of *E. coli* PBP 5 (Swiss Protein Database accession P04287) with *E. coli* PBP 6 (P08506) and PBP 6b (P33013), *H. influenzae* PBP 5 (P44466), and *S. typhimurium* PBP 6b (P37604). Conserved residues among all five PBPs are depicted in *green*. The active site serine is shown in *red*, the site of the mutation in sPBP 5′ is marked with by a @, and the cysteine residue in PBP 5 that reacts with sulfhydryl reagents is marked by a (#). The secondary structure assignments are shown below. The *dashed line* represents the disordered region 74–90. The first three residues and the last six residues (the latter of which are non-native and a result of the genetic construct) of sPBP 5′ have been omitted for clarity.

hydrogen bonding network (34), there are no visible water molecules in the immediate vicinity of the active site. However, further refinement and higher resolution data of sPBP 5′ may be necessary to firmly establish the presence or absence of potential active site water molecules.

Structural Homology of sPBP 5′ and TEM-1 β-Lactamase

One of the most outstanding features of the sPBP 5′ structure is the similarity of domain 1 with the fold of Class A β-lactamases, as represented by TEM-1 (35) and PC1 (36). Notably, this structural similarity is considerably more pronounced than previously reported PBP structures, namely the *Streptomyces* R61 D,D-peptidase (37) and PBP 2x from *Streptococcus pneumoniae* (38). The main chain atoms in the 209 residues of domain 1 of sPBP 5′ composing the common elements of secondary structure of penicillin-interacting proteins can be superimposed onto the PC1 β-lactamase fold (36) with

an r.m.s. deviation of 2.7 Å and the TEM-1 β-lactamase (39) fold with an r.m.s. deviation of 2.5 Å.

The similarity of domain 1 of sPBP 5′ and TEM-1 β-lactamase is shown in Fig. 5. The most significant differences between the two structures are 1) the N-terminal helix of TEM-1 is replaced by an extended chain in sPBP 5′, 2) the disordered region between residues 74 and 90 in sPBP 5′ is visible in TEM-1 as a small helix with connecting loops, 3) the extended loop (colored *blue* in Fig. 4, of sPBP 5′ has a slightly different conformation compared with its counterpart in TEM-1, the so-called Ω loop, and 4) in sPBP 5′ the connection between helices α8 and α9 contains a large β hairpin, whereas the equivalent connection in TEM-1, between helices α9 and α10, is direct.

A comparable degree of similarity with Class A β-lactamases was also observed in the recently determined structure of the *Streptomyces* K15 D,D-transpeptidase (40). In fact, the K15 PBP
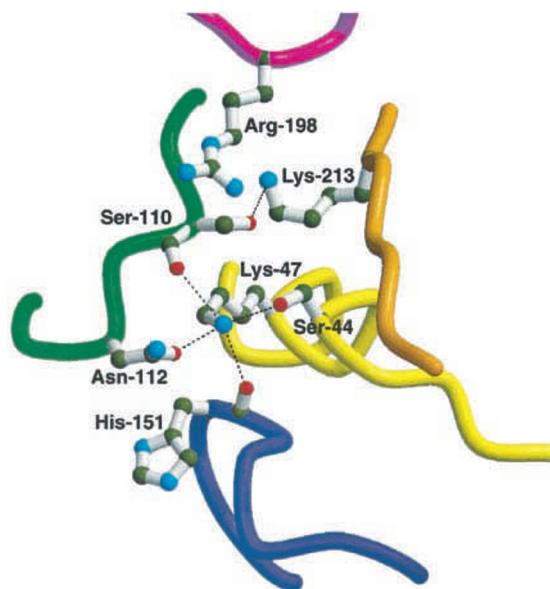
FIG. 4. **Active site architecture of sPBP 5′.** The active site is formed by five structural elements (colored *yellow*, *green*, *blue*, *purple*, and *orange*). Potential hydrogen bonds are denoted by the *dashed lines*. Note the orientations of the imidazole side chain and backbone carbonyl group of His-151 and the position of Arg-198. This figure was produced using MOLSCRIPT (51).

and sPBP 5′ are close structural relatives. Domain 1 of sPBP 5′ can be superimposed onto the K15 PBP structure with an r.m.s. deviation of 1.2 Å between common main chain atoms (212 residues). The main differences of note are that the part of the K15 PBP structure equivalent to the disordered region in sPBP 5′ (residues 74–90) is ordered and that the β7-β8 hairpin is considerably longer in the K15 PBP structure (β2c-β2d), generating a four-stranded β sheet on the surface of the K15 PBP. Unlike most other PBPs, the K15 PBP does not contain a traditional hydrophobic transmembrane anchor. Thus, it has been proposed that the β2c-β2d hairpin promotes the association of the K15 PBP with the cell membrane (40), which may explain its longer length.

The active site residues of sPBP 5′ and TEM-1 β-lactamase were aligned by the program LSQKAB (26) (Fig. 6). Ser-44, Lys-47, Ser-110, Asn-112, and Lys-213 are all spatially conserved with the corresponding residues in TEM-1 β-lactamase, again emphasizing the extensive homology between these two proteins. Although the extended Ω-like loop at the lower region of the active site of sPBP 5′ is similarly positioned to the Ω loop of TEM-1, there are significant conformational differences between the two. This is important because in Class A β-lactamases, the Ω loop contains two residues, Glu-166 and Asn-170, that are critical for the rapid hydrolysis of the acyl-enzyme complex (41, 42). By analogy, the Ω-like loop in PBP 5 (residues 147–157) may also contain similar residues responsible for deacylation, thus explaining the high β-lactamase activity observed in wild-type PBP 5 (see "Discussion").

DISCUSSION

Here we report the structure of a soluble, mutant form of PBP 5′ solved to 2.3-Å resolution by x-ray crystallography. The structure of sPBP 5′ reveals two domains, a penicillin-binding domain and a domain of unknown function. The fold of the penicillin-binding domain is highly similar to Class A β-lactamases, further emphasizing the close evolutionary relationship between these two classes of penicillin-interacting proteins.

Catalytic Function—PBP 5 is a serine-based D-alanine carboxypeptidase that is functionally similar to the well studied

family of serine proteases. Although both PBP 5 and the serine proteases proceed through formation of an acyl-enzyme intermediate followed by deacylation of the acylated enzyme, they have evolved distinctly different catalytic mechanisms. The close structural similarity of sPBP 5′ with Class A β-lactamases suggests a common mechanism of acylation by β-lactam antibiotics for the two classes of enzymes. In the light of the structure of PBP 5′, the potential roles in catalysis of the conserved active site residues of PBP 5 can now be discussed.

Acylation of PBP 5 with β-Lactam Antibiotics and Peptide Substrates—The acylation reaction comprises four steps: formation of the non-covalent complex, nucleophilic attack, tetrahedral intermediate formation, and collapse to the acyl-enzyme. Mutational evidence has shown that, at least for β-lactam antibiotics, a positive charge at position 213 is crucial for formation of the acyl-enzyme complex (33), suggesting that Lys-213 (of the KTG triad) interacts with the carboxylate group on both β-lactam antibiotics and peptide substrates. Interestingly, the equivalent residue in β-lactamases, Lys-234, has been proposed to stabilize the transition state (43, 44). Since in our structure the ε-amino group of Lys-213 interacts via potential hydrogen bonds with the hydroxyl group of Ser-110 and the carbonyl group of Asn-107, an alternative role of this residue may be simply to maintain the correct active site architecture rather than to interact with substrate directly. It is interesting to note that mutation of Lys-213 to arginine has no effect on penicillin binding and hydrolysis yet abolishes CPase activity (33). Such a mutation would increase the distance between two key components of the active site, β9 and the C-terminal end of α4, by approximately 1 Å. This may lower the binding affinity for peptide substrates, which presumably have a larger binding footprint without affecting the smaller binding site for penicillin.

Acylation starts by nucleophilic attack of the active site Ser-44 (22) on the amide bond of the peptide substrate or β-lactam ring. In serine proteases, the nucleophilicity of the serine residue is activated by the so-called "charge-relay" system involving a histidine and aspartic acid residue (45). In our structure it is difficult to assess which of the surrounding residues enhance the nucleophilicity of Ser-44. One possibility is that the amino group of Lys-47, which is within hydrogen-bonding distance of the Ser-44 hydroxyl, acts as a general base. For this to occur, however, the active site environment must promote the deprotonated state of the ε-NH_2 group, requiring a reduction in its pK_a of approximately 3 pH units. This might be achieved via its hydrogen-bonding interactions with Asn-112 and the carbonyl groups of His-151 and Ser-110 (Fig. 4). An alternative possibility is that the nucleophilicity of Ser-44 may be enhanced by the dipole moment of the helix α2. The role of the helix dipole has recently been suggested to increase the nucleophilicity of the active site cysteine in β-ketoacyl-acyl carrier protein synthase III, a bacterial enzyme that catalyzes a Claisen condensation in type II fatty acid synthesis (46).

It is interestingly to note that one characterized mutation, D175N, which abolishes CPase activity and decreases acylation by 50-fold (19), probably acts indirectly by perturbing the precise arrangement of the active site rather than having a direct role in catalysis as previously suggested. Our structure shows that the effect of this mutation is to break a hydrogen bond between the side chains of Asp-175 and Tyr-52, located at the C-terminal end of helix α2, more than 20 Å from Ser-44. That such a subtle change has such a large impact on activity is evidence that the precise positioning of the N-terminal end of α2, which contains Ser-44 and Lys-47, is critical for catalysis.

The developing negative charge on the carbonyl oxygen of the tetrahedral intermediate is likely stabilized by an oxyanion
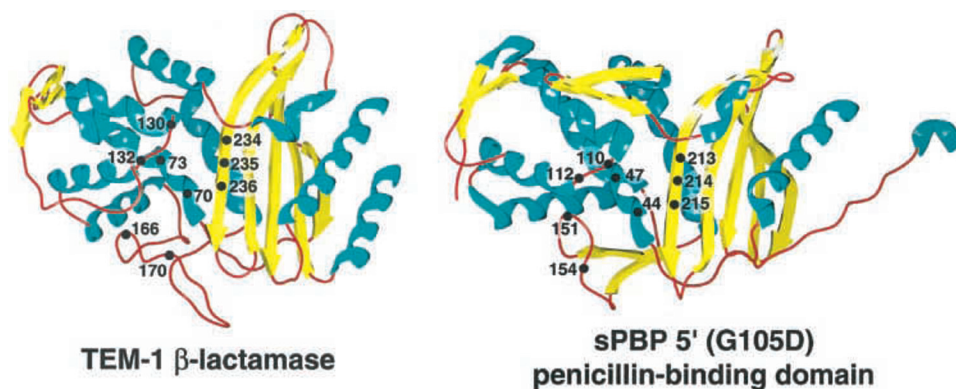
FIG. 5. **Structural homology of TEM-1 β-lactamase and the penicillin-binding domain of sPBP 5′.** The view of sPBP 5′ is similar to that shown in Fig. 4. The penicillin-binding domain of sPBP 5′ is comprised of residues 1–265. The positions of active site residues are shown by a ● along with their residue numbers. This figure was produced using the program SPOCK (available on the World Wide Web).
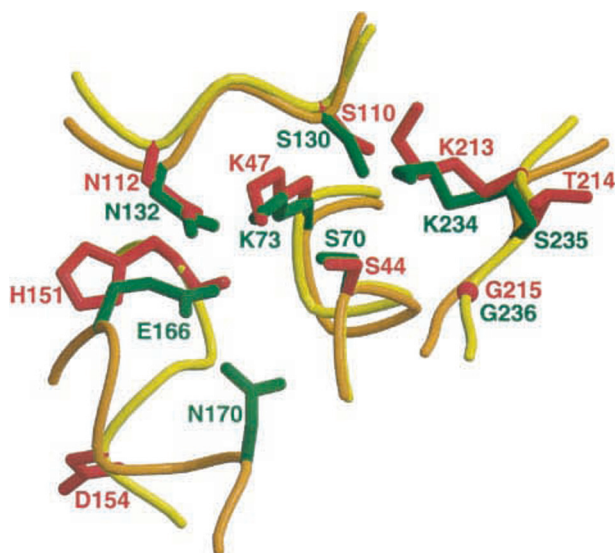

FIG. 6. **Alignment of the active site residues of sPBP 5′ and TEM-1 β-lactamase.** The active site residues of sPBP 5′ and TEM-1 β-lactamase (39) were aligned with the program LSQKAB (26). Backbone residues from sPBP 5′ are depicted in *orange*, and active site amino acids are shown in *red*. In TEM-1 β-lactamase, backbone residues are *yellow*, and active site amino acids are *green*. The carbonyl group of His-151 is also shown. This figure was produced using MOLSCRIPT (51).

hole similar to that proposed for many other enzymes, including serine proteases, β-lactamases, and other PBPs. In PBP 5′ the oxyanion hole is potentially formed by backbone amide groups of residues 214 and 216 from β9 and Ser-44 on α2. Arg-198 is positioned above the active site and may also help stabilize the intermediate.

Hydrolysis of the Acyl-Enzyme Complex—The close structural overlap of PBP 5′ with Class A β-lactamases suggests that the relatively high deacylation rate of the β-lactam-bound PBP 5 may be mediated by the loop equivalent to the Ω loop in Class A β-lactamases. In the latter, two residues on this loop, Glu-166 and Asn-170, are intimately involved in the rapid deacylation of the acyl-enzyme complex (42, 47). In particular, Glu-166 is believed to activate a conserved water molecule that attacks the carbonyl of the acyl-enzyme (41, 48). By analogy, residues in the Ω-like loop of PBP 5 may also position a catalytic water molecule that attacks the acyl-enzyme complex. Candidate residues from the Ω-like loop include His-151 and Asp-154, both of which are conserved in other CPases (Fig. 3) and one of which, His-151, is close to the active site (Fig. 4). However, in our structure of the deacylation-defective PBP 5′,

neither of these side chains is sufficiently close to the active site to interact directly with substrate or potential catalytic water molecules (Fig. 4). An alternative mechanism for hydrolysis of the acyl-enzyme complex is that the backbone carbonyl moiety of His-151, which in our structure is hydrogen-bonded to Lys-47 (Fig. 4), participates in deacylation simply by favorably orienting a hydrolytic water molecule. This is supported by the spatial equivalence of carbonyl group of His-151 in PBP 5′ with the carboxyl group of Glu-166 in TEM-1 (Fig. 6).

Further evidence that the Ω-like loop in PBP 5′ may indeed be involved in deacylation comes from studies of deacylation-defective forms of PBP 5. In the G105D mutant, Gly-105 (small) is replaced by aspartate (charged and bulky), which may disrupt the packing of helix α4 with the adjacent 74–90 loop and cause the apparent flexibility of the latter observed in our crystal structure. In both Class A β-lactamases and the K15 D,D-transpeptidase, the equivalent loop is ordered and packs against the counterparts of helices α4, α5, and the Ω-like loop in sPBP 5′. A second deacylation-defective PBP 5 is obtained through modification of Cys-115 by *para*-chloromercuribenzoate in the wild-type enzyme (18). This residue is located on helix α5 and packs into the space between α2 and α4. Introduction of such a bulky group would doubtless perturb this close packing and may also affect the conformation of the adjacent 74–90 loop. Thus it appears that a decrease in deacylation may result from changes in the specific region of the structure containing α4, α5, the 74–90 loop, and the Ω-like loop. In the structure of wild-type PBP 5, it will be interesting to note whether the 74–90 loop is more ordered and indeed whether the conformation of the Ω-like loop is altered as a result.

Relationship of sPBP 5′ to β-Lactamases—The structural homology between the *Streptomyces* R61 D,D-peptidase and PC1 β-lactamase was noted as early as 1986 (11, 12), but the similarity between sPBP 5′ and TEM-1 β-lactamase is even more pronounced. A comparable degree of similarity to Class A β-lactamases also has been observed with the *Streptomyces* K15 D,D-transpeptidase (40). It has been suggested that each of the different classes of β-lactamases have evolved from various classes of PBPs (49). Our data are entirely consistent with this hypothesis.

The main structural difference between the penicillin binding domain of sPBP 5′ and Class A β-lactamases is in the sequence and conformation of the Ω loop, perhaps suggesting that Class A β-lactamases evolved directly from a PBP 5-like CPase. This would be logical because CPases already had a relatively efficient hydrolysis mechanism for peptide substrates. By incorporating two new amino acids on the Ω loop and by removing residues specific for CPase activity, β-lacta-

mases evolved a highly efficient hydrolysis mechanism and at the same time altered their specificity toward β-lactam antibiotics and away from peptide substrates.

Role of Domain 2—The two-domain structure of PBP 5, in which catalytic activity resides in domain 1, is consistent with previous genetic studies showing that deletion of the protein after residue 263 results in an enzyme with near wild-type CPase activity and β-lactam antibiotic affinity (50). This, however, leaves the role of domain 2 unclear. One possibility is that this domain mediates interactions with other cell wall-synthesizing enzymes to recruit PBP 5 to areas of active cell wall synthesis. Indeed, the all β structure of this domain may facilitate such interactions through hydrogen bonding across β strands. In *E. coli*, the lytic transglycosylase, MltA, interacts with several PBPs as well as the scaffolding protein, MipA (8), suggesting the existence of a cell wall-synthesizing complex, of which PBP 5 may be a part. Alternatively, domain 2 may function simply as a linker to position the active site in domain 1 closer to the peptidoglycan layer, where it can interact with cell wall peptides.

Conclusion—By solving the crystal structure of a deacylation-defective mutant, we have obtained the first structural information for PBP 5. PBP 5 shares the same fold and has a common active site architecture with the well studied Class A β-lactamases. Inspection of this structure suggests that Lys-47 may act as the general base to promote the nucleophilicity of Ser-44 during acylation. In contrast, the mechanism of deacylation is less clear. However, solving the wild-type PBP 5 structure and comparing it to PBP 5′ should provide significant insight into how PBP 5 catalyzes hydrolysis of the acyl-enzyme complex. These studies are in progress.

REFERENCES

1. Ghuysen, J. M. (1988) *Rev. Infect. Dis.* **10,** 726–732
2. Tipper, D. J., and Strominger, J. L. (1965) *Proc. Natl. Acad. Sci. U. S. A.* **54,** 1133–1141
3. Ghuysen, J. M. (1991) *Annu. Rev. Microbiol.* **45,** 37–67
4. Spratt, B. G. (1975) *Proc. Natl. Acad. Sci. U. S. A.* **72,** 2999–3003
5. Matsuhashi, M., Tamaki, S., Curtis, S. J., and Strominger, J. L. (1979) *J. Bacteriol.* **137,** 644–647
6. Amanuma, H., and Strominger, J. L. (1980) *J. Biol. Chem.* **255,** 11173–11180
7. Denome, S. A., Elf, P. K., Henderson, T. A., Nelson, D. E., and Young, K. D. (1999) *J. Bacteriol.* **181,** 3981–3993
8. Nelson, D. E., and Young, K. D. (2000) *J. Bacteriol.* **182,** 1714–1721
9. Bush, K., and Sykes, R. B. (1984) in *Antimicrobial Drug Resistance*, pp. 1–31, Academic Press, Inc., New York, NY
10. Joris, B., Ghuysen, J.-M., Dive, G., Renard, A., Dideberg, O., Charlier, P., Frere, J.-M., Kelly, J. A., Boyington, J. C., Moews, P. C., and Knox, J. R. (1988) *Biochem. J.* **250,** 313–324
11. Samraoui, B., Sutton, B. J., Todd, R. J., Artymiuk, P. J., Waley, S. G., and Phillips, D. C. (1986) *Nature* **320,** 378–380
12. Kelly, J. A., Dideberg, O., Charlier, P., Wery, J. P., Libert, M., Moews, P. C., Knox, J. R., Duez, C., Fraipont, C., Joris, B., Dusart, J., Frere, J.-M., and Ghuysen, J.-M. (1986) *Science* **231,** 1429–1431
13. Ghuysen, J.-M., and Dive, G. (1994) in *Bacterial Cell Walls*, pp. 103–129, Elsevier Science Publishers B. V., Amsterdam
14. Pratt, R. F., and Govardhan, C. P. (1984) *Proc. Natl. Acad. Sci. U. S. A.* **81,** 1302–1306
15. Martin, M. T., and Waley, S. G. (1988) *Biochem. J.* **254,** 923–925
16. Amanuma, H., and Strominger, J. L. (1984) *J. Biol. Chem.* **259,** 1294–1298
17. Nicholas, R. A., and Strominger, J. L. (1988) *J. Biol. Chem.* **263,** 2034–2040
18. Curtis, S. J., and Strominger, J. L. (1978) *J. Biol. Chem.* **253,** 2584–2588
19. vanderLinden, M. P., deHaan, L., Dideberg, O., and Keck, W. (1994) *Biochem. J.* **303,** 357–362
20. Pratt, J. M., Jackson, M. E., and Holland, I. B. (1986) *EMBO J.* **5,** 2399–2405
21. Kustu, S. G., and Ames, G. F. L. (1974) *J. Biol. Chem.* **249,** 6976–6983
22. Nicholas, R. A., Ishino, F., Park, W., Matsuhashi, M., and Strominger, J. L. (1985) *J. Biol. Chem.* **260,** 6394–6397
23. Nicholas, R. A., and Strominger, J. L. (1988) *Rev. Infect. Dis.* **10,** 733–738
24. Otwinowski, Z., and Minor, W. (1997) *Methods Enzymol.* **276,** 307–326
25. Frere, J. M., Ghuysen, J. M., and Perkins, H. R. (1975) *Eur. J. Biochem.* **57,** 353–359
26. Collaborative Computation Project (1994) *Acta Crystallogr. Sec. D* **50,** 760–763
27. deLaFortelle, E., and Bricogne, G. (1997) *Methods Enzymol.* **276,** 472–494
28. Abrahams, J. P., and Leslie, A. G. W. (1996) *Acta Crystallogr. Sec. D* **52,** 30–42
29. Jones, T. A., Zhou, J. Y., Cowan, S. W., and Kjeldgaard, M. (1991) *Acta Crystallogr. Sec. A* **47,** 110–119
30. Laskowski, R. A., MacArthur, M. W., Moss, D. S., and Thorton, J. M. (1993) *J. Appl. Crystallogr.* **26,** 283–291
31. vanderLinden, M. P., Mottl, H., and Keck, W. (1992) *Eur. J. Biochem.* **204,** 197–202
32. Holm, L., and Sander, C. (1995) *Trends Biochem. Sci.* **20,** 478–480
33. Malhotra, K. T., and Nicholas, R. A. (1992) *J. Biol. Chem.* **267,** 11386–11391
34. Matagne, A., Lamotte-Brasseur, J., and Frere, J.-M. (1998) *Biochem. J.* **330,** 581–598
35. Rhazi, N., Galleni, M., Page, M. I., and Frere, J. M. (1999) *Biochem. J.* **341,** 409–413
36. Herzberg, O., and Moult, J. (1987) *Science* **236,** 694–701
37. Kelly, J. A., Knox, J. R., Moews, P. C., Hite, G. J., Bartolone, J. B., Zhao, H., Joris, B., Frere, J. M., and Ghuysen, J. M. (1985) *J. Biol. Chem.* **260,** 6449–6458
38. Pares, S., Mouz, N., Petillot, Y., Hakenbeck, R., and Dideberg, O. (1996) *Nat. Struct. Biol.* **3,** 284–289
39. Jelsch, C., Mourey, L., Masson, J. M., and Samama, J. P. (1993) *Proteins* **16,** 364–383
40. Fonzé, E., Vermeire, M., Nguyen-Distèche, M., Brasseur, R., and Charlier, P. (1999) *J. Biol. Chem.* **274,** 21853–21860
41. Adachi, H., Ohta, T., and Matsuzawa, H. (1991) *J. Biol. Chem.* **266,** 3186–3191
42. Lewis, E. R., Winterberg, K. M., and Fink, A. L. (1997) *Proc. Natl. Acad. Sci. U. S. A.* **94,** 443–447
43. Ellerby, L. M., Escobar, W. A., Fink, A. L., Mitchinson, C., and Wells, J. A. (1990) *Biochemistry* **29,** 5797–5806
44. Brannigan, J., Matagne, A., Jacob, F., Damblon, C., Joris, B., Klein, D., Spratt, B. G., and Frere, J. M. (1991) *Biochem. J.* **278,** 673–678
45. Fersht, A. R. (1985) *Enzyme Structure and Mechanism*, 2nd Ed., pp. 406–407, W. H. Freeman and Co., New York
46. Davies, C., Heath, R. J., White, S. W., and Rock, C. O. (2000) *Structure Fold. Des.* **8,** 185–195
47. Guillaume, G., Vanhove, M., Lamotte-Brasseur, J., Ledent, P., Jamin, M., Joris, B., and Frere, J. M. (1997) *J. Biol. Chem.* **272,** 5438–5444
48. Strynadka, N. C., Adachi, H., Jensen, S. E., Johns, K., Sielecki, A., Betzel, C., Sutoh, K., and James, M. N. (1992) *Nature* **359,** 700–705
49. Massova, I., and Mobashery, S. (1998) *Antimicrob. Agents Chemother.* **42,** 1–17
50. vanderLinden, M. P., deHaan, L., and Keck, W. (1993) *Biochem. J.* **289,** 593–598
51. Kraulis, P. J. (1991) *J. Appl. Crystallogr.* **24,** 946–950